



# Design of Solar Powered Automatic Change-Over Bill-Board for a Location in Umuahia

<sup>1\*</sup>Ugwu, H.U. and <sup>2</sup>Ogbonnaya, E.A.

<sup>1</sup>Department of Mechanical Engineering, Michael Okpara University of Agriculture, Umudike, Umuahia, Abia State, Nigeria.

<sup>2</sup>Department of Mechanical/Marine Engineering, Niger Delta University, Wilberforce Island, Bayelsa State, Nigeria.

**Abstract** - A solar powered automatic change over billboard (ACOB) was designed to meet the demand of advertising agencies, save cost and improve bill display capacity using locally available materials. The improvement from the use of a generator to solar, incorporating a motor, leads to a display capacity of four bills on a single billboard stand. With the motor transmitting a corresponding torque to the shaft and the gear assembly, the bills printed on vinyl sheet (flex banner) affixed at the rectangular prism panel bars were displayed and a changeover initiated, as controlled through the circuit timer. To conceptualize the study towards adapting solar as the power source, a cue was taken from an already existing electrical-powered system at Federal Medical Centre (FMC) Umuahia utilizing a generating set. Through this design, a solar powered ACOB with a display time of 120 seconds and a change over time of 5 seconds for a daily operation of 10 hours was achieved. For optimum bill display capacity, a solar panel with an output voltage of 18V appropriately configured to charge a 12V standard nickel-cadmium deep cycle solar battery was required. From the study, it indicated that an actual battery capacity of 22.4Ah and a storing current of 2.24A were required for the solar panel. It was also shown that a wind pressure of 0.192N/m<sup>2</sup> impinging on the billboard of weight 1128N producing a wind force of 0.167N were adequate for its stabilization, if erected.

**Keywords** - solar powered ACOB, improved advertisement capacity, gear-powered mechanism, energy and cost saving, dc motor transmission

## 1. INTRODUCTION

A billboard (sometimes called a hoarding in the United Kingdom and many other parts of the world) is a large outdoor advertising structure (a billing board) typically found in high traffic areas and cities, especially alongside busy roads (Henderson and Robert, 1986). Billboard presents a large advertisement to passing pedestrians and drivers typically showing large ostensibly witty slogan (text) and visual (pictures) displays. They are highly visible in the top designated market areas, stadium route and big cities. A billboard is a medium employed among other media for relaying information to the public. Agencies such as the government, commercial corporations, non-governmental organizations, religious groups and individuals or groups, employ this medium to inform the general public on various issues ranging from government projects, individual or group prospects, company advertisement (such as show-casing of new or improved products) and/or general public awareness. The billboard if erected has the potential of relieving these agencies and individuals of the drudgery experienced in advertising, reduce cost of procuring traditional billboards and their associated heavy maintenances,

enhance the environmental standard of living of people, and the attendant problems associated with the use of private generating sets with heavy fuel consumption rates.

In view of these, an improvement on the design of an already existing electrical to solar powered ACOB and how it could be developed was considered and consolidated in this study. The technology of displaying four bills, two on each side of a single billboard at the same time is novel since it has not been done especially in Nigeria. The existing billboards such as the non-automated mechanical billboard (or simply, the traditional billboard) and some electronic powered billboards investigated, have the capacity of displaying at a time, only one or two bills. This design however, brings the possibility of a display capacity of four bills (two on each side) on one billboard stand. This was made possible by the incorporation of a powered motor, gear and shaft arrangement, automated by an electric timer circuit. Hence, the employment of this design will bring about reduction in the cost of building or designing more traditional billboards for more display of bills. It will also result in the decongestion of the cities and highways by the traditional billboards, and add glamour and aesthetic to the environment. Moreso, advertising agencies stand to benefit from this improvement, with the possibility of displaying more bills on the billboard stand, and thus add more value to the national income

\*Corresponding author Tel: +234-80-64245409  
Email: [ubadyke2001@yahoo.com.au](mailto:ubadyke2001@yahoo.com.au)



from the displayed bills (Robert, 1979; Henderson and Robert, 1986; Rank, 2001).

Basically, an improvement of the non-automated traditional billboard led to the design and development of an electrical powered ACOB, which makes use of electricity for its operational system. Since these electrical powered ACOB relied on electricity, many agencies and companies would want their own electronic billboards to stay lit throughout the nights and day. However, these electronic billboards had to be near the grid (mostly unavailable) or connected to a generator (with huge running cost and maintenance) for their lighting purposes. It is with these obvious constraints that this newly designed system was hypothetically conceived to be made solar-powered.

In terms of solar energy production and availability of solar radiation in Nigeria, sun's insolation is readily available and abundant especially at Umuahia location and its environs. Umuahia situated on latitude 5°31'55"N and longitude 7°29'9"E at an elevation of 121m high, receives a minimum and maximum values of 2.6 and 4.3Kwh of solar radiation, respectively, representing long term monthly and yearly averages over the period 1985-2004 (Nwokocha et al., 2012). Thus, solar energy is clearly one of the most promising prospects of generating power in Nigeria since its generation is inexhaustible and the earth receives more energy from the sun than is consumed by mankind in a year. Hence, the solar energy when harnessed would be used for various applications. One of the greatest utilization is the technology of generation of solar electricity by photovoltaic, PV (Ugwu, 2011). This technology is simple, environmentally friendly, and cheaper to maintain since there is no moving parts involved. The only consumable source of energy is the sun utilized as fuel. In consonance with these, this paper therefore aims at showing that solar powered billboards when integrated with automatic changeovers would have the capacity for displaying more bills on a single billboard, would be cost effective and energy efficient compared to the conventional counterpart systems for power supply and advertisement.

## 2. DESIGN CONCEPTS AND APPROACH

### 2.1 The Concept of the Design

Figure 1 presents an isometric view of the billboard designed with the component parts labeled as represented in table 1. The design consists of series of rectangular panel bars made of light weight material (mild steel panel) of dimensions (L x W x H): 104cm x 19cm x 182cm with a supporting base of dimensions 61cm x 5cm x 5cm in length, width and height, respectively. A motor is incorporated to turn the panel bars while the support stands made of strong mild steel

material, form the base on which the billboard is mounted. The bills to be relayed or displayed are printed on vinyl sheet or flex banner, which are then cut to sizes and affixed on the faces of the rectangular prism panel bars. In this way, as the solar panels are rotated by the motor, four unique bills are displayed at different time intervals one after the other. This technique is thought to be more effective as the motor that actuates the display while rotating, draws attention of the passer-by to the message being displayed. The billboard has a combination of spur gear arrangement keyed to two roller shafts for the rotating changeover of the tarpaulin/flex material affixed at the rectangular prism panel bars in which the display bills are printed. One of the gears in connection to the (main) driving shafts is in mesh with the gear attached to the electric motor (Shighley et al., 2004). The electric motor itself is powered by solar energy using solar panel being controlled by a circuit timer that determines the "on and off" conditions of the motor.

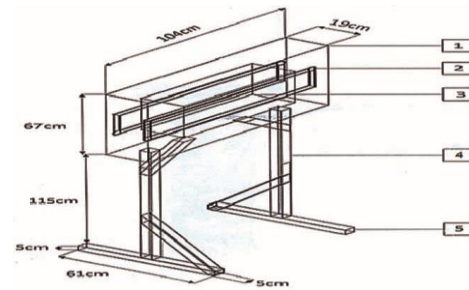


Fig. 1: An isometric view of the billboard (Assembling drawing)

Table 1: The components of the billboard designed as labeled in figure 1

S/N	Components	Quantity
1	Over-hanging support	2
2	Square-shaped bar (front)	1
3	Square-shaped bar (back)	1
4	Billboard stand	2
5	Base support	2
Others: Not shown in the figure 1		
6	Shaft	4
7	Bearings	8
8	Solar panel	1

A major modification attributed to in this design, is an improved display capacity of four bills employing both the front and back sides of the bill board for display purpose. The rotational movement of the electric motor transmits a rotational force to the driving shaft for the rotating changeover of the tarpaulin fixed on the rectangular prism panel bars to display on the side of the



board. By employing an idler gear, an equivalent rotational force is transmitted to the driving shaft of the other side of the board. Each driving shaft in consequence, has a supporting tensional shaft for both sides of the billboard. With this arrangement, each pair of the shafts is able to tension the tarpaulin/flex material end-joined-display sheet in order to display a total of four bills, composing of two, each on each side.

## 2.2 Principle of Operation and Technical Approach to the System

The solar powered ACOB designed consists basically of a D.C. electric motor, solar panel made from wafers of high-grade silicon (solar SX 146 solarex) with a cell size of 0.1016 x 0.1016m (4 x 4 inches). The operating voltage is 18.0 volts with a peak power of 220 watts. The system operates at a current of 12.22 Amperes, with a resistance of 1.47 Ohms in a series cell connection of 40 numbers of cells, made of polycrystalline silicon material. Incorporated to the design are four spur gears, four roller shafts, circuit timer, polythene tarpaulin, eight ball roller bearings, and a 12 volt battery.

In addition, the solar array on a PV cell (solar panel) can only generate D.C. For this reason, a special D.C. powered motor was utilized which enabled the electricity produced by the solar array to vary as the solar input (solar radiation) varies. This necessitated the use of regulators and the employment of deep charge solar batteries to store the electricity generated. The deep cycle batteries obviously are required for power (storage) and its supply to the billboard so as to provide for the periods of cloudy and raining days that may be envisaged. Thus, a PV array or the panel provided, charges the battery during the day of relatively good sunshine through a charge controller which was employed to regulate the current from the solar panels, prevent the battery from being overcharged or undercharged, and from back-feeding into the solar panel at night. In this regard, the regulator in the charging circuit thus, maintains a charging voltage of 12 volts for the battery when the output from the solar panel is greater than 14 volts. A nickel-Cadmium (NiCd) deep cycle solar battery was selected over the lead acid battery for the design because it lasts longer, can be completely flattened and stored without damage, do not exhibit the sudden death characteristic of the lead acid batteries, and are less susceptible to degradation due to cycling. The NiCd battery also delivers greater long-term value by being able to endure more charge/discharge cycles, lasts much longer, and discharges more current before needing to be recharged (Solar-Online, 2014).

Consequently, the battery powers a D.C. motor while a second regulator was employed to ensure that the motor runs only within its rated range. This induces the

motor to transmit a corresponding torque to the shaft and the gear assembly, thus displaying the bill and initiating a changeover which is controlled through the circuit timer. The schematic of the circuit assembly for the power supply with other integrated component parts for powering the motor is as presented in figure 2. From the figure, the electric motor being powered by the solar energy from the sun, and controlled by the counter, sends an output to the circuit timer at the end of each counting cycle. This in turn, determines the “on and off” conditions of the motor, thus giving the billboard display pane, control over its bills’ change within a specified duration of time.

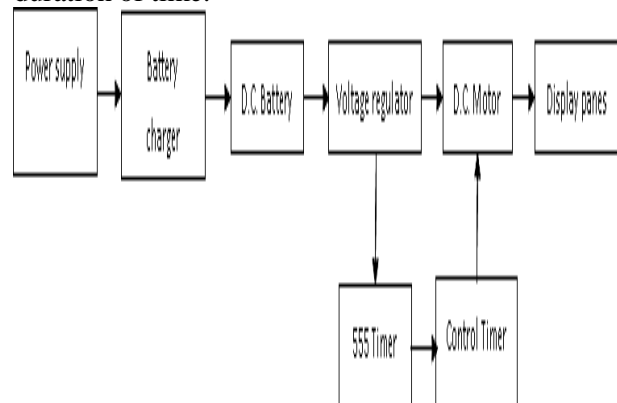


Fig. 2: Circuit for the supply of power

The timing control of this ACOB was realized through the use of two 555 timers configured both in astable and monostable mode operation. A 74ALS193 counter was integrated into the timing arrangement to give the billboard control over its change within a specified duration. The resistor-capacitor values of the astable mode timer was selected to make the output of the 555 timer deliver pulses which are square wave in form for every 19 seconds. This output thus, clocks the 74ALS193 counter, which on completion of its counting cycle sends an output to the monostable mode timer within a 2 minute interval. Consequently, the monostable mode timer delivers an output pulse whose duration lasts for a period long enough to drive the motor. This in turn, supplies power to a system of gear to bring about rotation of the square-shaped display bars. These are depicted as presented in figures 3 and 4.

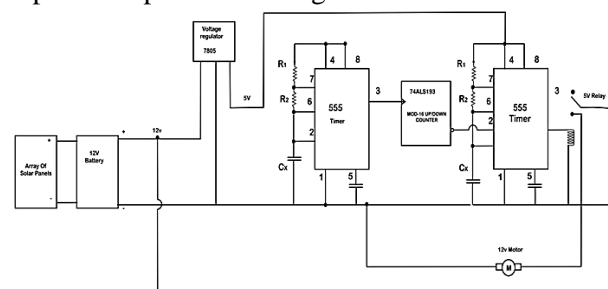


Fig. 3: The schematic diagram of the circuit and its integrated components for the supply of electricity and timing.

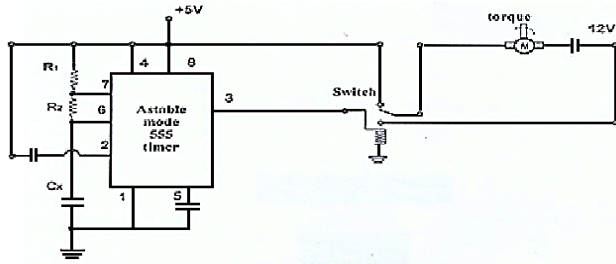


Fig. 4: The 555 timer circuit

### 2.2.1 The Counter (74ALS193 Module-16 Counter)

The digital counter 74ALS193 depicted in figure 5 presents a module-16 up/down counter which counts up to 16 clock pulses before resetting its outputs to zero (Hodge, 2004). This system of the setting are also interpreted and presented in table 2 as observed under  $\overline{TC}_u$  column. In the figure 5,  $CP_u$  = upward pulses;  $CP_D$  = downward pulses;  $\overline{TC}_u$  = upward output pin;  $\overline{TC}_D$  = downward output pin; P = input pulse; and Q = output counting pulse, respectively.

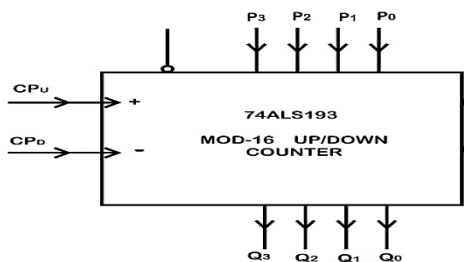


Fig. 5: 74ALS193 module-16 counter

Table 2: The digital counter (74ALS193 module-16 counter)

$CP_u$	$Q_0$	$Q_1$	$Q_2$	$Q_3$	$\overline{TC}_u$
1	0	0	0	0	1
2	1	0	0	0	1
3	0	1	0	0	1
4	1	1	0	0	1
5	0	0	1	0	1
6	1	0	1	0	1
7	0	1	1	0	1
8	1	1	1	0	1
9	0	0	0	1	1
10	1	0	0	1	1
11	0	1	0	1	1
12	1	1	0	1	1
13	0	0	1	1	1
14	1	0	1	1	1
15	0	1	1	1	1
16	1	1	1	1	0
17	0	0	0	0	1

It will be noted that the  $\overline{TC}_u$  output pin on the 74ALS193 as Hodge (2004) stated is normally HIGH and would be momentarily driven LOW at the last count

before resetting to zero, while the output from the  $\overline{TC}_u$  is used to trigger the monostable mode timer at the end of the counter sequence.

## 3.0 DESIGN ANALYSIS

### 3.1 The Timing Calculations of the 555 Clocking Timers

According to Onoh (2006), the capacitor,  $C_{XA}$  for astable mode 555 circuit timer from figure 6 is calculated using:

$$T = t_1 + t_2 \quad (1)$$

$$t_1 = 0.693 R_B C_{XA} \quad (2)$$

$$\text{and } t_2 = 0.693 (R_A + R_B) C_{XA} \quad (3)$$

$$\text{But: Frequency, } f = \frac{1}{T} \quad (4)$$

$$\text{and Duty cycle, } D_{cycle} = \frac{t_2}{T} \times 100 \% \quad (5)$$

Substituting equations (2) and (3) in (1) gives:

$$T = 0.693 C_{XA} (2R_B + R_A) \quad (6)$$

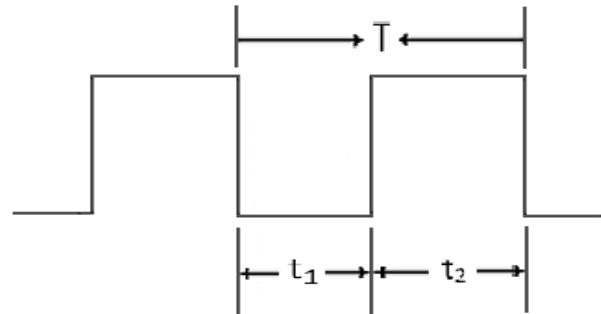


Fig. 6: The Waveform Configuration of an Astable Mode 555 Timer

Based on figure 3, the following parameters for the astable and the monostable mode 555 circuit timers are established as:  $R_A$  = Resistor 1 of the astable 555 timer = 1k $\Omega$ ;  $R_B$  = Resistor 2 of the astable 555 timer = 5.5k $\Omega$ ;  $C_{XM}$  = Capacitance of the capacitor for the monostable mode timer; T = Time for the clocking = 19 seconds; and Numbers 1, 2, ..., and 8 = Pin or hole links, respectively. Thus, from equation (6), the capacitance of the capacitor,  $C_{XA}$  used for the astable mode timer is obtained as 2.28 $\mu$ f.

Similarly, from figure 3 based on Onoh (2006), the capacitance of the capacitor for the monostable mode 555 circuit timer,  $C_{XM}$  is calculated using:

$$T = 0.693 (R_1 + R_2) C_{XM} \quad (7)$$

As Onoh (2006) stated, the output from this stage is normally at 0 volt and would produce a high voltage output upon being triggered as represented in the waveform configuration of figure 7. Conversely, from equation (7), the capacitance of the capacitor,  $C_{XM}$  used for the monostable mode timer is obtained as 0.25 $\mu$ f. It will be noted that  $R_1$  and  $R_2$  according to Tocci (2008) are pre-settable resistors which are adjusted to give an accurate duration of motion to the square shaped display



bars. Thus, the output from the stage is fed to the D.C. motor through a 5volt relay in order to isolate the timer stage from the higher voltage D.C. motor stage.

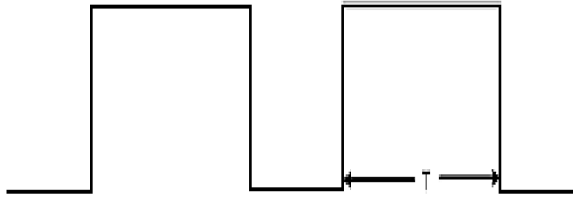


Fig. 7: The Waveform Configuration of a Monostable 555 Timer

### 3.2 Life Weight/Wind Forces Acting on the Billboard

Wind forces on structures and structural elements linking to the billboard result from the differential pressure due to such objects inhibiting the free flow of the wind. Since moving air has mass and velocity and thus kinetic energy, the billboard being placed on the wind path/direction transforms all or part of the kinetic energy of the wind into potential energy when the air is incidentally stopped or deflected, resulting to wind forces building up on the object. The increase in static pressure on the object (that is, the wind force, or wind load) based on Robert (1979) can be calculated from: Wind pressure,  $P_W = 0.00256 C_S V$  (pounds/ft<sup>2</sup>) ... (8)

where:  $P_W$  = Wind pressure (pounds per square foot);  $V$  = Assumed design wind velocity/speed (miles per hour) = 4.6km/hr or 1.28m/s = 2.86mph; and  $C_S$  = Non-dimensional shape factor (drag) co-efficient = 1.8 (for flat plates and most other stationary bodies), respectively. (Note: 1pound per square foot (lb/ft<sup>2</sup>) = 47.88 N/m<sup>2</sup> and 1 mile per hour (mph) = 0.4472 m/s).

It is to be noted also that the wind pressure relation (equation 8) as obtained in most literature cannot be applied directly in isolation without reference to its original British units (as used in this study) since it derived its roots from the imperial system of measurements. Hence, the conversion of the constant (0.00256) from the British standard unit to Standard International (metric) unit, thus, is given (ASCE Standard, 2003) as:

$$\text{Constant} = \frac{1}{2} \left[ \frac{0.0765 \text{ lb/ft}^3}{32.2 \text{ ft/s}^2} \right] * \left[ \frac{\text{mile}}{\text{hr}} * \frac{5280 \text{ ft}}{\text{mile}} * \frac{1 \text{ hr}}{3600 \text{ s}} \right]^2 = 0.00256$$

$$\text{Equivalent to: Constant} = \frac{1}{2} \left[ \frac{1.225 \text{ kg/m}^3}{9.81 \text{ m/s}^2} \right] * \left[ \frac{\text{m}}{\text{s}} \right]^2 * \frac{9.81 \text{ N}}{\text{kg}} = 0.613$$

The constant 0.00256 (or 0.613 in SI unit) based on ASCE Standard (2003), reflects the mass density of air for the standard atmosphere, i.e. temperature of 59°F (15°C) and sea level pressure of 29.92 inches of mercury (101.325kpa), and dimensions associated with wind speed in mph (m/s). Hence, the numerical constant (0.00256) should be used in its imperial standard and subsequently converted to its metric equivalent, except where sufficient weather data are available to justify a different value of this constant as applied in equation (8) for a specific design application (ASCE Standard, 2003). Thus, from equation (8):

$$\text{Wind pressure, } P_W = 0.00256 * 1.8 * 2.86 = 0.01318 \text{ lb/ft}^2 \equiv \frac{0.01318 \text{ lb} * 4.4482 \text{ N} * \text{ft}^2}{\text{ft}^2 * \text{lb} * 0.304782 \text{ m}^2} = 0.1924 \text{ N/m}^2$$

### 3.3 Mounting (Installation) and Stability of the Billboard

Figures 8 shows the front view section of the billboard, while table 3 presents the description, and the dimensions for the labeled parts in figures 1 and 8 respectively, and the determination of their respective areas and volumes taken from their centroids; where:  $y$  = the distance of the strip from the centre of gravity (Cg).

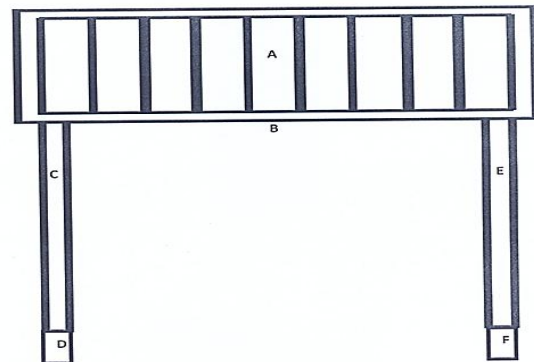


Fig. 8: Front View Section of the Billboard

Table 3: Description, dimensions and calculations for parts labelled in figures 1 and 8

Parts	Description	Dimensions: L x W (cm)	Area: $A_{bb}$ (cm <sup>2</sup> )	Strip distance (y) from Cg (cm)	Strip volume: $A_y$ (cm <sup>3</sup> )
A	Square-shaped display bars	104 x 67	6968	155.5	1083524
B	Overhanging support	104 x 5	520	122.5	63700
C, E	Billboard stands	115 x 5 each	$575 * 2 = 1150$	$62.5 * 2 = 125$	71875
D, F	Base supports	5 x 5 each	$25 * 2 = 50$	$2.5 * 2 = 50$	125
<b>Total</b>			<b>8688</b>		<b>1219224</b>



Since the system is symmetrical on the y-axis, it is evident from table 3 that the  $C_g$  of the billboard will lie at:  $\frac{Ay(cm^3)}{A_{bb}(cm^2)} = 140.3cm$  or  $1.403m$  from the ground, while the weight of the billboard acts vertically from its  $C_g$ . Conversely, the wind forces acting horizontally on the billboard of mass  $115kg$  under a gravitational pull of  $9.81m/s^2$  are determined using the force vectors diagram represented in figure 9.

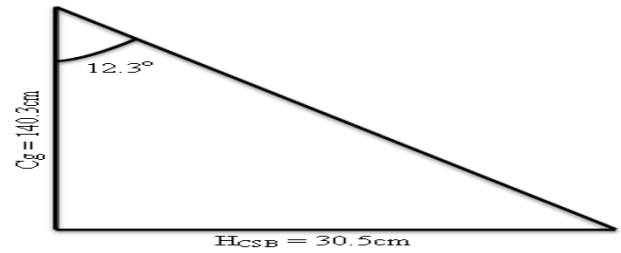


Fig. 10: Force Components Acting On the Support Base of the Billboard

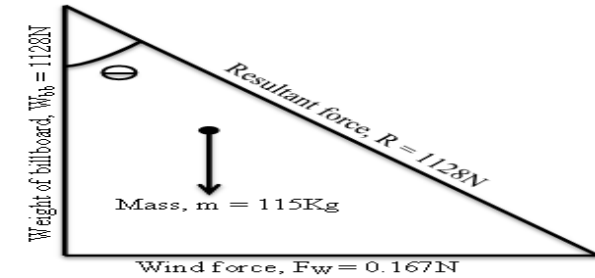


Fig. 9: Force components acting on the billboard

Thus: Weight of the billboard,  $W_{bb} = \text{mass of the billboard} \times \text{gravitational acceleration/intensity} = 115kg \times 9.81m/s^2 = 1128.15N$  approx.  $1128N$  (9)  
Conversely, from figure 9 and table 3:

Wind force,  $F_W = \text{Wind pressure, } P_W \times \text{Area of billboard, } A_{bb} = 0.1924N/m^2 \times 0.8688m^2 = 0.167N$  (10)

Hence: Resultant force,  $R = \sqrt{W_{bb}^2 + F_W^2} = 1128N$  (11)

The value of  $1128N$  for the resultant force obtained which equals the weight of the billboard as calculated implies that the billboard will continue to remain steady and stable as long as the resultant force,  $R$  continues to act within the length of the support stand.

### 3.3.1 Other considered parameters of the billboard designed:

#### 1. Angle of Displacement

From trigonometry, based on figure 9:  $\cos \theta = \frac{W_{bb}}{R} = 1$ ; and thus,  $\theta = 0^\circ$ . This implies that the billboard will continue to remain stable with the subjected wind force provided its displacement angle maintains zero degrees, and the wind force on the billboard large mass becomes substantially negligible.

#### 2. Maximum Angle of Displacement for the Billboard

With an average of  $30.5cm$  (Horizontal component for the support base:  $H_{CSB}$ ) length of  $61cm$  (figure 1), and the calculated  $C_g$  of  $140.3cm$ , the maximum angle of displacement for stability for the billboard is obtained. Thus, from trigonometry based on figure 10:  $\tan \theta = \frac{H_{CSB}}{C_g} = 0.21739$ ; and thus,  $\theta = 12.3^\circ$ . This implies that the billboard can only be displaced when the resultant force exceeds this value of  $12.3^\circ$  corresponding to its maximum angle; beyond which, stability would no longer be guaranteed.

### 3.4 Square-Shaped Bar Display, Shafts, Gear and Bearings

As illustrated in figures 11 and 12, the solar powered ACOB designed has a combination of spur gear arrangement keyed to two roller screw threaded shafts for the rotation of the changeover of the square-shaped display panel bar. The square-shaped display panel bars (figure 11) to which the displayed bills would be printed, affixed or glued were cut in eight equal sizes with the same dimensions ( $18cm \times 18cm \times 67cm$ ) in length, width and height respectively. The gear in connection to the main driving shaft was in mesh with the gear in connection to the electric motor (figure 12). The rotational movement of the electric motor transmits a corresponding rotational force to the driving shaft. This subsequently rotates the changeover of the square-shaped display bar made of light mild steel material of high quality and durability. The choice for the selection of the tarpaulin/flex banner of high ductile and tensile quality for the design was due to the length capability for tension to be transmitted (Shigley et al., 2004).

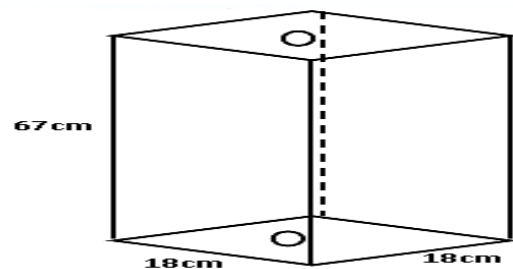


Fig. 11: Isometric View of the Square-Shaped Display Panel Bar

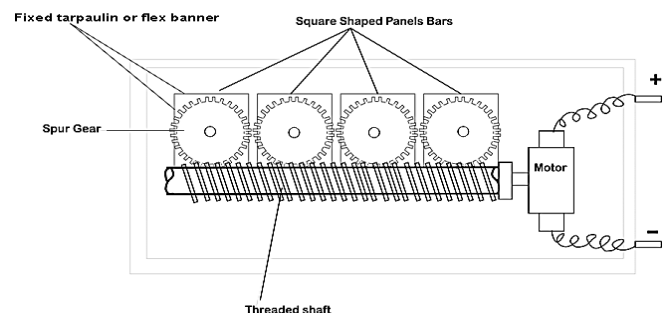


Fig. 12: Sectional View of the Spur Gear, Threaded Screw Roller and Square-Shaped Display Panel Bars.



### 3.4.1 Power transmitted by the Pinion

The system of gear assembly for the billboard represented in figure 13 was employed for the design. Because the billboard was designed to operate for a maximum of 10hours daily at steady load, the table 4 was utilized to select corresponding Service Factor  $S_F$  values that would adequately match the system of gears and the pinion assembly. The tangential tooth load transmitted on the pinion according to Khurmi and Gupta (2009) was obtained using the relation:

$$W_T = \frac{P}{V} \times S_F = \frac{60P}{\pi DN} \times S_F = F^t \quad (12)$$

where:  $W_T$  = permissible tangential tooth load in Newton;  $P$  = power transmitted in watt = 80W or 0.08KW;  $S_F$  = Service factor = 1.00. Also,  $V$  = pitch line velocity in m/s =  $\frac{\pi DN}{60}$  (13)

where:  $N$  = speed in rpm = 76.2rpm; and  $D$  = diameter of the pinion = 8cm or 80mm, respectively. Thus, the permissible tangential tooth load,  $W_T$  is calculated as 0.2506KN or 251N approximately.

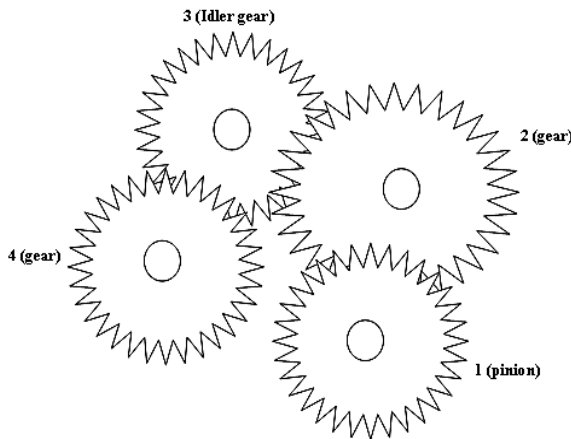


Fig. 13: System of Gears for the Billboard

Table 4: The Service factor values of gears and pinion

S/N	Type of load	2-5 hours per day	8-10 hours per day	24 hours per day
1	Steady	0.80	1.00	1.25
2	Light shock	1.00	1.25	1.54
3	Medium shock	1.25	1.54	1.80
4	Heavy shock	1.54	1.80	2.00

### 3.4.2 Load Transmitted To Gear

The recommended pressure angle,  $\theta$  for gear 2 in the system of gears of figure 13 based on the table of gear system proposed by the American Gear Manufacturing Association is given as  $20^\circ$  (Shighley et al., 2004).

Hypothetically, this is represented in the force diagram shown in figure 14.

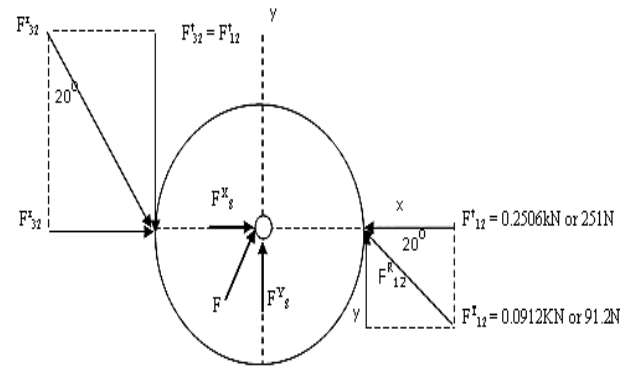


Fig. 14: Force diagram of the transmitted load on the gear assembly

From trigonometry:  $\tan 20^\circ = \frac{F_{12}^t}{F_{12}^r} = \frac{F_{12}^t}{0.2506}$  and  $F_{12}^t = 0.2506 \times 0.3640 = 0.0912\text{KN}$  or 91.2N

Conversely:  $\cos 20^\circ = \frac{F_{12}^t}{F_{12}^r}$  and  $F_{12}^r = \frac{F_{12}^t}{\cos 20^\circ} = \frac{0.2506}{0.9397} = 0.2667\text{KN}$  or 266.7N

Since gear 3 is an idler gear (figure 13), and transmits no force to any shaft, the tangential force acting on gear 2 from gear 3 is equivalent to  $F_{12}^t$ . Hence:  $F_{12}^t = F_{32}^t = 0.2506\text{KN}$ ;  $F_{32}^r = 0.0912\text{KN}$  and  $F_{32}^r = 0.2667\text{KN}$ , respectively. From figure 14, the component of the shaft reaction in the x and y directions are obtained as:  $F_S^x = -[F_{32}^t + F_{32}^r] = -0.2506 - 0.0912 = -0.3418\text{KN}$ ; And  $F_S^y = -[F_{32}^r + (-F_{32}^t)] = -0.2506 + 0.0912 = -0.1594\text{KN}$ ; thus: Resultant force on shaft,

$$F_{RS} = \sqrt{(F_x)^2 + (F_y)^2} = 0.3771\text{KN}$$
 or 377.1N

### 3.4.3 Selection of Gears

Considering gears 1 and 2 of the gear assembly of figure 13, the pinion 1 is to transmit the required torque to the gear 2. Since the pinion and the gear are made of the same material, the pinion was taken to be weaker than the gear in this design. This design condition was considered to be key factor to enable the gears withstand the maximum stress required (Stock, 1993). From the force analysis on the gears, and with an allowable static stress,  $\delta_o$  of  $240\text{N/mm}^2$  for a treated forged carbon steel (Khurmi and Gupta, 2005) as presented in table 5, the conditions of the pinions were determined using equation (14) and the Velocity Ratio (VR) obtained as 1.269; thus:

$$VR = \frac{T_g}{T_p} \quad (14)$$

where:  $T_g$  = no of gear teeth = 33;  $T_p$  = no of teeth of the pinion = 26; speed of rotation of the gear = 76.2rpm;  $D_g$  = diameter of the gear = 80mm; and pressure angle =  $20^\circ$ , respectively.



Table 5: Values of allowable static stress of some materials

S/N	Materials	Allowable static stress: $\delta_0$ (N/mm <sup>2</sup> )
1	Cast iron, ordinary	56
2	Cast iron, medium grade	70
3	Cast iron, highest grade	105
4	Cast steel, untreated	140
5	Forge carbon steel, case hardened	126
6	Forge carbon steel, untreated	140 - 210
7	Forge carbon steel, treated	220 - 240
8	Alloy steel, case hardened	350
9	Alloy steel, heat hardened	455 - 472
10	Phosphor bronze	84

Source: Khurmi and Gupta (2005)

Also, the recommended gear module (GM) was obtained using the relation:

$$\text{Gear module, GM} = \frac{\text{Diameter of gear}}{\text{Number of gear teeth}} = \frac{D_g}{T_g} = 2.42 \text{ mm} \quad (15)$$

Conversely, the Pitch line velocity ( $P_{LV}$ ) was obtained as:

$$P_{LV} = \frac{\pi \times N_p \times D_p}{60} = 0.3192 \text{ m/s} \quad (16)$$

Pitch line velocity ( $P_{LV}$ ) was operating at a velocity less than 12.5m/s (Khurmi and Gupta, 2005), the Velocity factor ( $V_F$ ) thus becomes:  $V_F = \frac{3}{3 + 0.3192} = 0.9038$

Consequently, the Teeth-form factor for the pinion,  $Y_p = 0.154 - \frac{0.9038}{T_p}$  (17)

Also, the Teeth-form factor for the gear,  $Y_g = 0.154 - \frac{0.9038}{T_g}$  (18)

Hence, these teeth-form factors are calculated as:  $Y_p = 0.1192$  and  $Y_g = 0.1266$ , while the stress parameters for the pinion and the gear, respectively are obtained as:  $\delta_p = \delta_{op} \times Y_p = 28.61 \text{ N/mm}^2$ ; and  $\delta_g = \delta_{og} \times Y_g = 30.38 \text{ N/mm}^2$ .

### 3.4.4 Load transmitted by the pinion, $L_p$

The load transmitted by the pinion,  $L_p$  was calculated using the relation:

$$L_p = \delta_{op} V_F \pi m Y_p b \quad (19)$$

Conversely, the power transmitted by the pinion,  $P_p$  is obtained using:

$$P_p = L_p \times P_{LV} \quad (20)$$

where:  $\delta_{op} = 240 \text{ N/mm}^2$ ;  $V_F = 0.9038$ ;  $m = 2.4 \text{ mm}$ ;  $Y_p = 0.1192$ ; and  $b = 0.1 \text{ mm}$ .

Thus, the load ( $L_p$ ) and the power ( $P_p$ ) transmitted by the pinion, were calculated as 19.5KN and 6224.4W, respectively. Since the power transmitted by the gear (motor) of 80W is less than the calculated value for the pinion of 6224.4W, it implies that the selected gear is appropriate for the forces acting on the gears.

### 3.4.5 Bearing Selection

In order to select the most suitable ball bearing, the basic radial load on the bearing ( $L_{RB}$ ) was calculated; and subsequently multiplied by the Service factor ( $K_{SFB}$ ) value for the selected radial ball bearing (table 6) to get the design basic dynamic radial load capacity ( $L_{DRC}$ ). Thus, the radial load on bearing ( $L_{RB}$ ) due to power transmitted was obtained using:

$$L_{RB} = W_N \sin \phi = F_{21}^T \sin \phi \quad (21)$$

where:  $\phi = \text{pressure angle of pinion teeth} = 20^\circ$ ; and  $F_{21}^T = W_N = 0.0912 \text{ KN}$

Table 6: The Service factor ( $K_{SFB}$ ) values for radial ball bearings

S/N	Type of service	Service factor ( $K_{SFB}$ )
1	Uniform and steady load	1.0
2	Light shock load	1.5
3	Moderate shock load	2.0
4	Heavy shock load	2.5
5	Extreme shock load	3.0

Source: Khurmi and Gupta (2005)

Hence, for a single deep groove bearing, the radial load ( $L_{RB}$ ) was obtained as 0.0312KN. According to Khurmi and Gupta (2005), the Basic static/dynamic load rating ( $L_{BSR}$ ) was obtained applying

$$L_{BSR} = W \left( \frac{B_{RL}}{10^6} \right)^{\frac{1}{K_{SFB}}} = L_{RB} \left( \frac{B_{RL}}{10^6} \right)^{\frac{1}{K_{SFB}}} \quad (22)$$

where:  $W = L_{RB} = \text{equivalent dynamic loading} = 0.0312 \text{ KN}$ ;  $K_{SFB} = \text{service factor} = 3$  for the worst extreme shock load that may be applied (table 6); and  $B_{RL} = \text{bearing rating life} = 1440 \times 10^6 \text{ hrs}$  representing 5 years of use at 10 hours of daily operation. Therefore, the Basic static/dynamic load rating ( $L_{BSR}$ ) was calculated as 0.352KN. This implies that a bearing of radial load of 0.0312KN with the capacity of 0.352KN may be selected for the design. However, to ensure adequate factor of safety, a bearing of higher capacity (5.65KN) with a



bearing number of 304, having an internal diameter,  $\delta_i$  of 25.2mm and an external diameter,  $\delta_o$  of 55.5mm respectively was chosen for this design.

### 3.4.6 Shaft Design

The shaft as a rotating component of the billboard system is used to transmit power from the motor to the spur gears. The power from the motor is delivered to the shaft by some tangential force and the resultant torque (twisting moment) set up within the shaft. This permits the power to be transferred to the system of gears keyed to the shaft. For this design, a carbon steel material was selected and used for the shaft because of its high strength, good machineability, low notch sensitivity factor, good heat treatment properties, higher wear resistant properties, high rigidity factor and stiffness (Khurmi and Gupta, 2005). These mechanical properties of the steel selected and their recommended values for shock and fatigue are as presented in tables 7 and 8 respectively.

Table 7: Mechanical Properties of Steel Considered For the Shaft Selection

Inclination standard designation	Ultimate tensile strength (MPG)	Yield strength (MPG)
40C8	560-670	320
45C8	610-700	350
50C4	640 -760	370
50C12	700 Min	390

Source: Khurmi and Gupta (2005)

Table 8: Recommended values considered for shock and fatigue factors for bending ( $K_m$ ), and torsion ( $K_t$ )

S/N	Nature of load	Bending ( $K_m$ )	Torsion ( $K_t$ )
<b>1</b>		Stationary shaft:	
<b>a</b>	Gradual applied load	1.0	1.0
<b>b</b>	Suddenly applied	1.5-2.0	1.5-2.0
<b>2</b>		Rotating shaft:	
<b>a</b>	Gradually applied or steady load	1.5	1.0
<b>b</b>	Suddenly applied load with minor shocks only	1.5-2.0	1.5-2.0
<b>c</b>	Suddenly applied load with heavy shock	2.0-3.0	1.5-3.0

Source: Khurmi and Gupta (2005)

For the design of the threaded screw shaft (either by cold or hot working), the American Society of Mechanical Engineers' Standard code was adopted (Shigley et al., 2004). These standard code parameters were used in the analysis of the forces acting on the shaft members and their housing.

### A. Analysis of the Forces Acting On the Shaft Members and the Housing

Figure 15 presents the forces acting on the shaft members and their housing. From the figure: Sum of forces =  $T_1 + T_2 = F^t_{gear}$  (23)

where:  $T_1$  and  $T_2$  = tensions on tarpaulin; and  $F^t_{gear}$  = tangential force on the gear.

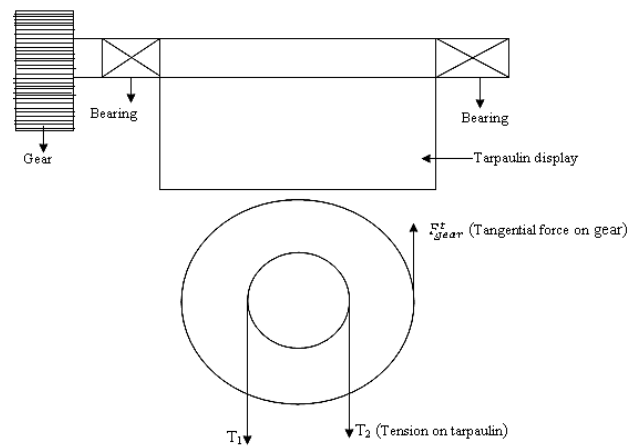


Fig. 15: Forces acting on the shaft members and housing

The torque on the shaft,  $T_{shaft} = F^r_{shaft} \times R_s$  (24)

Also, the shaft diameter for the design,  $D_s = 52mm$ ; and the shaft radius,  $R_s = 26mm$ , while  $F^r_{shaft} \equiv F_{RS} = 377.1N$  (as obtained).

Therefore, from equation (24), the Torque on the shaft,  $T_{shaft}$  is obtained as 9804.6Nmm.

But:  $F^t_{gear} \equiv F^t_{12} = 0.2506KN$  or 251N (as obtained); hence, from equation (23):

$$T_1 + T_2 = 251 \quad (25)$$

$$\therefore T_2 = 251 - T_1 \quad (26)$$

Conversely:

$$T_{shaft} = (T_1 - T_2) R_s = 9804.6 = (T_1 - T_2) \times 26 \quad (27)$$

Hence:  $T_1 = 314.05N$  and  $T_2 = -63.05N$  (absolute value in tension).

### B. Force Analysis on Shaft A

Figures 16 and 17 represent respectively, the schematic analysis of the forces, and their resolutions, while figure 18 and table 9 illustrate the bending moment diagram, and the calculations of the bending moment diagram for the resolution of the forces acting on the shaft of the billboard. From table 9 and figure 18, it is evident that the maximum bending moment for the shaft



about point A is 64.8Nm. In the figures,  $R_A$  = reaction on bearing A;  $R_B$  = reaction on bearing B;  $T_t$  = torque on shaft; and  $W_s$  = weight of Shaft = 260N, respectively.

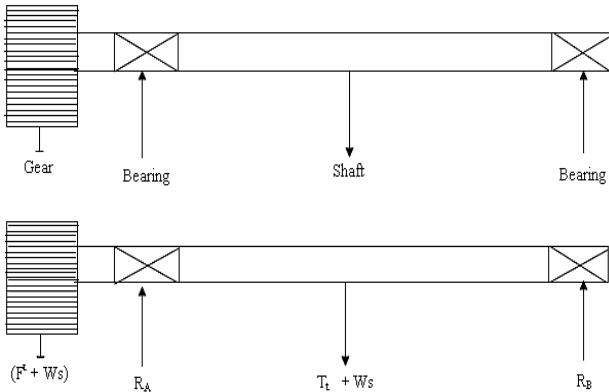


Fig. 16: Schematic Analysis of Forces on the Billboard Shaft

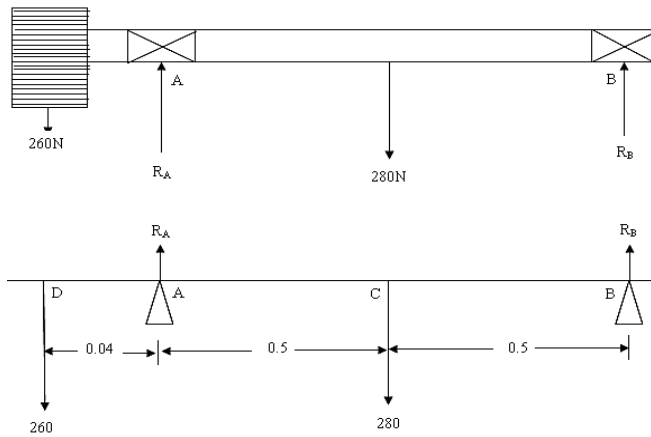


Fig. 17: Resolution of the Forces Acting On the Shaft of the Billboard

From Rajput (2006): Sum of upward forces = sum of downward forces; thus:

$$R_A + R_B = 260 + 280 = 540$$

Taking Moment about point A from figure 17 gives:  $(260 \times 0.04) + R_B \times 1 = 280 \times 0.5$

Hence:  $R_B = 129.6\text{N}$  and  $R_A = 410.4\text{N}$

Table 9: Bending Moment Diagram Calculation for the Resolution of the Forces Acting On the Shaft of the Billboard

Region	Bending moment
DA: (0.00 - 0.04)	$260 \times 0.04 = 104$
AC: (0.04 - 0.54)	$(410.4 \times 0.5) - (260 \times 0.54) = 64.8$
CB: (0.54 - 1.00)	$(410.4 \times 1.0) - (260 \times 1.04) + (280 \times 0.5) = 0$

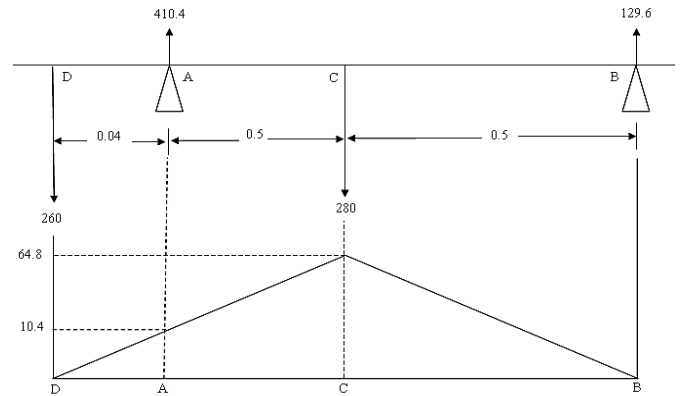


Fig. 18: The Bending Moment Diagram of the Forces Acting On the Shaft of the Billboard

Conversely, figures 19 and 20 present the force analysis on the shaft of the billboard, and the bending moment diagram respectively, while table 10 indicates the bending moment calculations of the respective forces acting on the shaft of the billboard about the point B. Similarly, from the force analysis of the figure 19:  $R_A + R_B = 280$

Taking moment about point A yields:  $(280 \times 0.5) - (R_B \times 1) = 0$ ; hence:  $R_B = 140\text{N}$  and  $R_A = 140\text{N}$

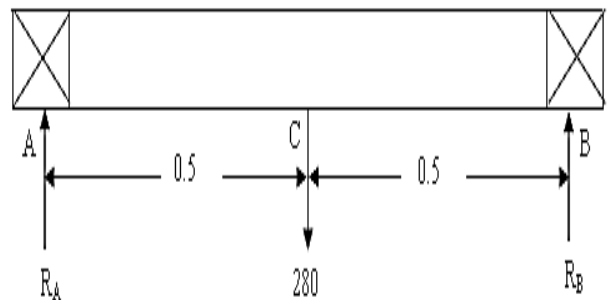


Fig. 19: Resolution of the Forces Acting On the Shaft of the Billboard

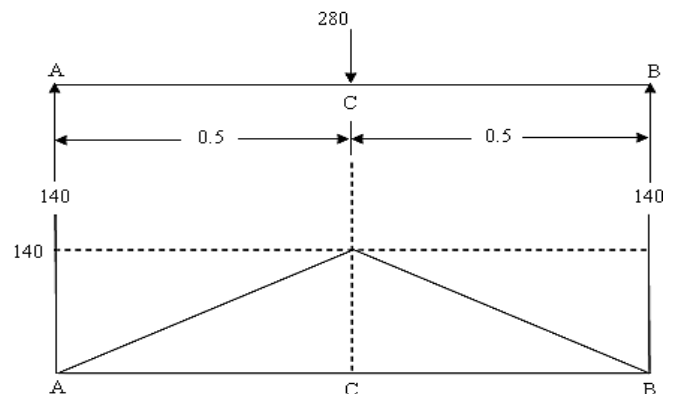


Fig. 20: The Bending Moment Diagram of the Forces Acting On the Shaft of the Billboard



Table 10: Bending Moment Diagram Calculation for the Resolution of the Forces Acting On the Shaft of the Billboard

Region	Bending moment
AC: 0.0 – 0.5	140 x 0.5 = 70
CB: 0.5 – 1.0	(140 x 1.0) – (280 x 0.5) = 0

From the figure 20, it is obvious that the maximum bending moment on the shaft of the billboard about the point B occurred at 140Nm. Hence, the bending moment of the forces about the point B on the shaft evidently, is higher with a value of 140Nm; and was used as the shaft design factor. Based on Khurmi and Gupta (2005) and Ryder (1973), the equivalent twisting moment, ( $T_e$ ) of the hollow screw shaft for the design is given as:

$$T_e = \sqrt{M^2 + T^2} = \frac{\pi}{16} \tau d_o^3 (1 - K^4) \quad (28)$$

where:  $T_e$  = equivalent twisting moment; M = maximum bending moment acting on the shaft = 140Nm or 140000Nmm; T = torque on the shaft (sum of forces on the shaft)  $\equiv F_{gear}^t = 251N$ ;  $\tau$  = permissible torsional (working) shear stress in tension on shaft; and  $K$  = design factor =  $\frac{d_i}{d_o}$  (as  $d_i$  = radius of inside diameter, and  $d_o$  = outside diameter of the shaft), respectively. Thus:  $T_e = \sqrt{140000^2 + 251^2} = 140000.225Nmm$

The Indian Standard Organization specified that the recommended design factor,  $K$  for transmitted torque is 0.94, and that for the torsional shear stress,  $\tau$  is 25Mpa (25N/mm<sup>2</sup>) respectively (Ryder, 1973). In-view of these and applying equation (28) yields:  $140000.225 = \frac{\pi}{16} \times 25 \times d_o^3 (1 - 0.94^4) = 1.0766d_o^3$  and  $d_o = 50.66mm$

Thus: Design factor,

$$K = 0.94 = \frac{d_i}{50.66} \text{ and } d_i = 47.62mm.$$

Hence, the required minimum shaft thickness,  $d_t = d_o - d_i = 3.04mm$ . To ensure adequate factor of safety based on the calculated values, an inside diameter,  $d_i$  of 52.0 mm and above, and an outside diameter,  $d_o$  of 55.0 mm and above, having the shaft thickness,  $d_t$  of 3.0 mm and above (i.e. 55.0 – 52.0) were used for the shaft design. This implies that the diametrial shaft thickness of 3.0 mm and above proposed, being greater than the minimum thickness calculated indicates that the shaft as used is suitable for the designed work.

### 3.4.7 Amperage Daily Requirement and Amperage of Solar Panel

The ampere-hour capacity rating of battery is employed to describe how much current or energy the battery to be used is required to supply or store for a given number of hours in use. The battery capacity in ampere-hour according to Gladstone and William (1993) can be calculated from:

$$\text{Ampere-hour} = \frac{\text{Power needed} \times \text{time of use} \times \text{power factor}}{\text{Battery voltage}} \quad (29)$$

where: the operation of the bill board = 10 hours/day (8am-6pm); powering time-off per display = 2 minutes (120sec); and powering time-on to turn bill = 5 seconds. But, a fraction of one period for every 2 minutes power-off and 5 seconds power-on in order to obtain an approximate daily hour in use was advocated for the design; hence:

$$\text{Fraction of one period} = \frac{\text{time-on period}}{\text{time-off period}} = 0.0417$$

Consequently, the time of use for a total of 10 hours daily operation becomes: 0.0417 x 10 hours = 0.42 hrs.

But: Motor rating power (power needed) = 80W; motor power factor = 0.008KW or 8W; and battery voltage = 12 volts; hence: Ampere-hour (Ahr) =  $\frac{80 \times 0.42 \times 8}{12} = 22.4 \text{ Ahr}$

Thus: Current requirement of battery per 10 hours of operation =  $\frac{\text{Ahr}}{\text{Time of operation}} = 2.24 \text{ Amperes}$

This implies that the solar panel required for the design should have an actual battery capacity of 22.4 Ahr and a storing current capacity of 2.24 Amperes which are just suitable for the amperage desired.

## 4. CONCLUSION AND RECOMMENDATIONS

### 4.1 Conclusion

The design of a solar-powered ACOB while taking a cue from an existing billboard powered from the national grid lines has been actualized. It is a viable and reliable alternative resource for an uninterrupted source of power for relaying, advertising and disseminating information to the general public. Economically, it is a very viable resource even though its initial cost would be high, but in the long run, it would be the most adoptable choice in terms of usage, cost effectiveness and maintenance. It requires no fuel but sun's insolation and little maintenance. In its modesty, the concept imbibed in this hypothetical design as investigated, shows remarkable improvement in the modification process of the existing electrical powered ACOB and/or traditional billboards to the present solar powered system.

From the design analysis and the bill of quantities undertaken at an overhead cost of 30%, the cost implication for the system was estimated at one hundred and ninety-two thousand, two hundred and five (N192,205.00) naira only, excluding cost due to labour and transportation, were it to be erected. The design if



erected, has the potential of relieving agencies (government, commercial corporations, religious groups, individuals and non-governmental organizations) of the drudgery experienced in advertising, reduce cost of procuring traditional billboards and their associated heavy maintenances, enhance the environmental standard of living of people, and the attendant problems associated with the use of private generating sets with heavy fuel consumption rates.

#### 4.2 Recommendations

The following recommendations are advocated for this design:

1. Government should provide strong financial support and backings for further research, technological and market development especially in the renewable energy (solar energy and PV technology) industries for the production of solar panels and deep solar storage facilities and devices.
2. A better visual (video) “satisfaction” as highlighted in the study should be incorporated in further design and other future modifications to enhance visualization; and
3. Proper and adequate policies and incentives which encourage the dissemination and commercialization of solar energy technology in Nigeria should be enacted and encouraged in order to reduce over dependence on supply from national grid-lines, and diversify our sole conventional petroleum energy resource base, for good integrated national energy mix.

#### ACKNOWLEDGEMENTS

The authors acknowledge with passion, the ingenuity and creativity of Mr. Ajaero, Chibunna of the Department of Mechanical Engineering, Michael Okpara University of Agriculture, Umudike in sourcing the relevant data for the design that assisted in the analysis.

#### REFERENCES

American Society of Civil Engineers (ASCE) Standard. (2003). Minimum Design Loads for Buildings and Other Structures, Structural Engineering Institute, SEI/ASCE 7-02, Revised second edition of ASCE 7-98, p.1-334.

Gladston, G.S. and William, G.S. (1993). “The dynamics of solar electric house”. Addison Wesley Longman Ltd; London.

Henderson, S.R. and Robert, O. M. (1986). “Billboard art”. San Francisco Chronical Books, 1986.

Hodge, M.D. (2004). “The concept of digital computer programming”. 2<sup>nd</sup> Revised edition. Macmillian Press Ltd, London, United Kingdom.

Khurmi, R.S. and Gupta, J.K. (2005). “Machine design”. Eurasia Publishing House (PVT) Ltd; Ram Nagar, New Delhi 110055, pp. 570 – 620.

Khurmi, R.S. and Gupta, J.K. (2009). “Theory of machines”. S. Chad and Company Ltd; Ram Nagar, New Delhi 110055.

Nwokocha, C.O., Chineke, T.C. and Fagbenro, A.B. (2012). Renewable energy potentials for Nigeria: Making the transition from oil and gas to solar, Prime Journal of Physical Science (PJPS), 1 (4): 31-39.

Onoh, G.A. (2006). “The principle of basic electrical engineering”, 6<sup>th</sup> Revised edition.

Rajput, R.K. (2006). “Strength of materials”. S. Chand and Company Ltd; Ram Nagar, New Delhi, 110055, p. 189 – 245.

Rank, S.G. (2001). Total estimate of monthly average daily global solar radiation in African, Nigerian Journal of Solar Energy (NJSE), 19 (1): 40-47.

Robert, K. L. (1979). “Structural Analysis and Design”. McGraw Hill Inc. United State of America.

Ryder, G.H. (1973). “Strength of materials”. The Macmillan Press Ltd; London.

Shighley, J.E., Mishchke, C.R. and Budynas, R.G. (2004). “Mechanical engineering design”, McGraw Hill, New York, p. 482-590.

Solar Online (2014). Solar system basics – How does solar power work? Accessed from [http://www.solaronline.com.au/solar\\_system\\_basics.html](http://www.solaronline.com.au/solar_system_basics.html) on 15 of April, 2014.

Stock, A. (1993). “Manual on gear box design”, Butter-Worth Heinemann Ltd; Linacre, Jordan Hill Oxford OX28DP.

Tocci, B.W. (2008). “Theory of integrated circuit and performance”, Butterworth Heinemann Ltd; New York.

Ugwu, H.U. (2011). Hypothetical adaptation of the design of stand-alone solar photovoltaic system as resource base substitute for optimal alternative energy production for remote residential application, International Review of Mechanical Engineering (IREME), 5 (7): 1340-1351.